JOURNAL OF SOLID STATE CHEMISTRY **141,** 570–575 (1998)
ARTICLE NO. SC988022

Ba_3AlO_4H: Synthesis and Structure of a New Hydrogen-Stabilized Phase

Baoquan Huang and John D. Corbett[1]

Ames Laboratory-DOE[2] and Department of Chemistry, Iowa State University, Ames, Iowa 50011

Received May 21, 1998; in revised form August 25, 1998; accepted September 7, 1998

The title compound and its deuteride were synthesized in high yield by sintering appropriate mixtures of $BaH_2(BaD_2)$, BaO and Al_2O_3 in welded Ta containers at 1100 °C under a hydrogen (deuterium) pressure of 600–700 torr. The structure was determined by a combination of single crystal X-ray and time-of-flight powder neutron diffraction means (orthorhombic *Pnma*, $Z = 4$, $a = 10.4911(9)$, $b = 8.1518(7)$, $c = 7.2399(6)$ Å for the deuteride). The compound contains nominal Ba^{2+} cations, AlO_4^{5-} complex anions and $H^-(D^-)$ anions. The hydride is bound in a strongly distorted barium octahedron while the tetrahedral AlO_4^{5-} anion is surrounded by eleven barium atoms in a peculiar polyhedral configuration. The HBa_6 octahedra are linked together by corner-sharing to form a three dimension framework with large voids defined by eight of the HBa_6 octahedra that are occupied by the tetrahedral AlO_4^{5-} anions. The structure is closely related in a hierarchical way to that of orthorhombic inverse perovskitic Ba_3GeO. © 1998 Academic Press

INTRODUCTION

Recently, we have systematically reexamined some compounds formed by the alkaline-earth metals (*Ae*) and the later main-group (*p*-block) elements because their formation, stoichiometry, and structure are controversial and incomplete. Many are complicated by hydrogen impurities in the *Ae* reagents (1). We have quantitatively synthesized a series of hydrogen-stabilized Zintl phases, such as Ae_5Pn_3H ($Pn =$ As, Sb, Bi), (formerly β-Yb_5Sb_3 type) (1, 2), Ae_5Tt_3H ($Tt =$ Si, Ge, Sn, Pb), Sr_5Tl_3H (Cr_5B_3 type) (3), $Ba_5Ga_6H_2$ (4), $Ba_{21}Tt_2O_5H_{24}$ ($Tt =$ Ge, Si), and $Ba_{21}Tr_2O_5H_{22}$ ($Tr =$ Ga, In, Tl) (5). These materials had initially been described as binary intermetallic compounds, such as eight examples of Ae_5Pn_3 (6), Sr_5Tl_3 (7), Ba_5Ga_6 (8), $Ba_{10}Ga$ (9), and ternary suboxides such as $Ba_{21}T_2O_5$ ($T =$ Ge, Si, Ga, In Tl) (10, 11) because hydrogen as an interstitial or anionic component had not been recognized or considered.

During attempts to synthesize a possible hydrogen-stabilized version of the suboxide $Ba_{17}Al_3O_7$ (12), we accidentally discovered the new phase Ba_3AlO_4H, which shows a close structural relationship to the orthorhombic inverse perovskite Ba_3GeO (13). Here we present its synthesis and structural definition by X-ray single-crystal and neutron powder diffraction means.

EXPERIMENTAL

Synthesis

Sublimed barium (Aldrich-APL, 99.99%), its binary hydride, and the product of the present studies are very sensitive to air and moisture, and they were therefore handled only in He- or N_2-filled glove boxes ($H_2O < 1$ ppm vol). Binary barium hydride was prepared from barium metal by reaction with hydrogen (600 torr, Matheson, 99.999%) at 800°C for 12 h. Barium deuteride was prepared in a parallel manner with D_2 (Matheson, 99.5%) instead of H_2. In this case, impurity hydrogen in the stock barium metal was first removed from Ba sealed in Ta by heating in high vacuum at 1100°C. Guinier X-ray powder patterns showed only the binary hydride (or deuteride) was formed. Barium oxide was prepared by decomposition of barium carbonate (Baker, 99.8%) in an open Ta container for 24 h at 1000°C under a dynamic vacuum ($\leq 10^{-5}$ torr). The Guinier X-ray pattern showed only the presence of BaO. The other materials used were Al (United Mineral and Chemical, 99.999%) and Al_2O_3 (Baker, 99.0%).

Red transparent single crystals of Ba_3AlO_4H were initially isolated from the product of a reaction loaded as $Ba_{17}Al_3O_7H_x$ that was heated at 1100°C and cooled at 20°C/h. A single crystal was also obtained during a synthesis in the ternary Ba–Ge–Al system that was contaminated by very small amounts of oxygen and hydrogen. It was later found that single-phase samples could be

---

[1] To whom correspondence should be addressed.

[2] The Ames Laboratory is operated for the U.S. Department of Energy by Iowa State University under Contract W-7405-Eng-82. The research was supported by the Office of Basic Energy Sciences, Materials Sciences Division, DOE. The U.S. Government's right to retain a nonexclusive royalty-free license in and to the copyright covering this paper, for governmental purposes, is acknowledged.

0022-4596/98 $25.00

synthesized from stoichiometric mixtures of BaH_2 or BaD_2, BaO and Al_2O_3 with an overall composition $Ba_3AlO_4H(D)$ (total amount: 500–2000 mg) that were thoroughly ground and welded in a Ta container under Ar. This was in turn placed in fused-silica tubing and connected to a high-vacuum source ($\leq 10^{-5}$ torr). The assembly was heated at 300°C for 4 h to remove some H_2O from the jacket, then charged with hydrogen or deuterium to 600–700 torr, heated to 1100°C, and held there for 12 h (under H_2 or D_2) followed by cooling at 20°C/h. The final quaternary product was a white powder that was extremely sensitive to air and gave a Guinier powder pattern that appeared to be single phase according to the powder pattern calculated after the structure had been solved. A 4.0-g deuteride sample was sealed under He into a gasketed vanadium cylinder with an inner diameter of 8 mm for the neutron diffraction experiment.

A Ta container was also loaded with ~ 500 mg of this Ba_3AlO_4D product, welded under Ar, and then heated to 1100 °C under high vacuum for 4 h followed by cooling to room temperature. The final product had a gray color, and the X-ray pattern indicated a mixture of $Ba_4Al_2O_7$ and $Ba_8Al_2O_{11}$ (14). A microscopic examination showed the product contained many small black particles, which were presumed to be Ba metal. ($8Ba_3AlO_4D \rightarrow 4Ba + 3Ba_4Al_2O_7 + Ba_8Al_2O_{11} + 4D_2$).

X-Ray Powder Diffraction

Guinier patterns were obtained from finely powdered samples mixed with NIST silicon ($a = 5.43088$ Å) with the aid of monochromatic Cu$K\alpha_1$ radiation ($\lambda = 1.54056$ Å). These were mounted between pieces of cellophane tape and held under forepump vacuum within an Enraf-Nonius Guinier camera. Cell parameters were refined from indexed lines and their 2θ values determined with the aid of a nonlinear fit to the positions of the standard Si lines.

X-Ray Single-Crystal Diffraction

Several crystals were sealed in thin-walled glass capillaries and checked for singularity by Laue photographs. Room temperature data were collected from one on a Rigaku AFC6R diffractometer (Mo$K\alpha$ radiation from a rotating anode and a graphite monochromator) with an ω–2θ scan mode for 2θ up to 50°. Three standard reflections measured every 150 reflections during the data collection did not change in intensity significantly. Statistical analysis of the intensity distribution showed primitive orthorhombic centrosymmetry, and the systematic absences $k + l = 2n + 1$ in $0kl$, $h = 2n + 1$ in $hk0$ indicated the unique space group D_{2h}^{16}-*Pnma*.

The structure was solved by direct methods via SHELXS (15). The atomic positions and thermal parameters were refined with the TEXSAN package (16) on a VAX station. Absorption corrections were found to be crucial for this compound because Ba is a strong absorber of Mo$K\alpha$ radiation ($\mu = 189.4$ cm^{-1}). The corrections were carried out according to ψ-scan curves for three strong reflections at different θ, and this gave isotropic convergence and a good heavy-atom model with $R(F) = 0.033$ and $R_w = 0.043$. A subsequent absorption correction by DIFABS (17) was applied in an attempt to locate the hydrogen atom. The orthorhombic structure according to the X-ray data and including one hydrogen atom with a fixed position from neutron diffraction studies was later refined anisotropically on F_o by full-matrix least-squares methods. A total of 543 reflections with $F_o > 3\sigma_I$ and 32 variables gave $R(F) = 0.021$ and $R_w = 0.023$. The ellipsoids were then notably smaller and more nicely spherical than before the second absorption correction. Some X-ray single-crystal data collection and refinement parameters are listed in Table 1. The structure factor data are available from J.D.C.

Neutron Powder Diffraction

The atomic parameters and isotropic displacement amplitudes for a deuteride sample were established with the aid of neutron powder diffraction data collected at room temperature on the Special Environment Powder Diffractometer (SEPD) at the Intense Pulsed Neutron Source (IPNS) facility at Argonne National Laboratory. The SEPD is a time-of-flight powder diffractometer with multidetector arrays at fixed scattering angles, and the high-resolution data from the $2\theta = 144.8°$ backscattering detector bank were used for this refinement. The powder data were refined by the Rietveld method (18) with the PC version of the General Structure Analysis System (GSAS) by Larson and Von Dreele (19), starting with the positional data from the X-ray study. The nuclear scattering lengths were taken from Ref. (20). The final refinement included data in the range $0.50 < d < 4.0$ Å (5252 profile points, 2865 reflections).

The heavy-atom structure from X-ray studies readily refined to reveal a single deuterium site in a distorted octahedral barium interstice. (The same position was deduced from X-ray data, but a second ghost peak of the same size was also present near Ba.) Preliminary refinements gave a D atom occupancy of 99.2(5)% (U_{iso} fixed), which was then fixed at unity. One impurity phase, BaO, was also observed, and its proportion and lattice parameter were included in the refinement; the relative amount was found to be 2.2(1)% (by weight). The background function was a cosine Fourier series with 12 coefficients. The other variables were as follows: two phase fractions, four lattice parameters, sixteen atomic positional parameters, and seven isotropic displacement parameters. The final conventional agreement indices were $R_p = 3.47\%$ and $R_{wp} = 5.22\%$ with a reduced χ^2 of 1.748. Some neutron data collection and refinement

TABLE 1
Crystallography and X Ray Refinement data for Ba_3AlO_4H

Crystal data	
Crystal size (mm), color	$\sim 0.15 \times 0.15 \times 0.15$; red, transparent
Crytal system	Orthorhombic
Space group, Z	*Pnma* (No. 62), 4
Lattice constants (Å)[a]	$a = 10.505(4)$ $b = 8.155(3)$ $c = 7.234(4)$
V(Å^3)	619.6(8)
d_{calc} (g/cm^3)	5.402
μ(Mo$K\alpha$) (cm^{-1})	189.35
Data collection	
Diffractometer	Rigaku AFC6R
Temperature (K)	296
Radiation, λ (Å)	Mo$K\alpha$, 0.709580
Scan type	ω–2θ
Reflections measured, $2\theta_{max}$	$+h$, $+k$, $\pm l$, 50°
Refinement	
Number of measured reflections	1248
Number of unique observed reflections ($I > 3\sigma_I$)	543
R(int)	0.020
Number of variables	32
Absorption correction	3 ψ-scans, DIFABS
Relative transmission coefficient range	0.922–1.00
$R(F_o)$, R_w[b] for $I > 3\sigma_I$	0.021, 0.023
ΔF_{max} peak, hole (e/Å^3)	0.97, -1.33

[a] Rigaku data.

[b] $R = \sum||F_o| - |F_c||/\sum|F_o|$, $R_w = [\sum(|F_o| - |F_c|^2/\sum wF_o^2]^{1/2}$, $w = \sigma_F^{-2}$.

parameters are listed in Table 2. The neutron diffraction patterns in Fig. 1 show the raw intensity data and, from top to bottom in each range, the background, the individual contributions from the main phase Ba_3AlO_4D and the impurity BaO, each with tick marks for the location of the reflections included, and the difference between the calculated and observed intensity profiles.

RESULTS AND DISCUSSION

Reactions among BaH_2 or BaD_2, BaO, and Al_2O_3 at the proper stoichiometry under a pressure of 600–700 torr H_2 or D_2 at 1100°C followed by slow cooling gave quantitative yields of Ba_3 $AlO_4H(D)$ according to Guinier patterns. This must be a gas–solid–solid reaction process since the product remained in powder form. Experiments showed that a thorough grinding of the starting materials is the key step in a high-yield synthesis. Single crystals were obtained only in the presence of excess BaH_2 or Ba metal as a flux. If the Ba_3AlO_4D product is heated again (in Ta) to 1100°C but under high vacuum, the D_2 is lost, and the decomposition gives Ba metal and, according to the powder pattern, two barium aluminates whose structures have not yet been determined. The Ba metal particles led to the gray sample color product.

The structure of Ba_3AlO_4H was refined from a combination of X-ray single-crystal and time-of-flight neutron power data. The final atomic coordinates, the isotropic-equivalent temperature factors, and their estimated standard deviations from both studies are listed in Table 3. The final neutron results are clearly more precise, and it is from these that the distance and angular data in Table 4 were obtained.

The compound crystallizes in a new structure type with orthorhombic symmetry, space group *Pnma*. The structure is made up of Ba^{2+} cations, AlO_4^{5-} complex anions, and isolated $D^-(H^-)$ anions as shown in two views in Figs. 2 and 3. The result is an orthorhombic distortion of a quasi-inverse perovskite type X_3AB brought about by the ordering of the three X (Ba^{2+}) cations, A (AlO_4^{5-}) anions, and B (D^-) anions, but not from a simple distortion because the AlO_4^{5-} anion is not a sphere. The Ba positions about deuterium are strongly distorted from octahedral geometry, as shown in Fig. 4, with Ba–D bond distances from 2.843(3) to 2.995(3) Å and cis Ba–D–Ba bond angles between 79.69(7) and 106.00(7)°. The deformed DBa_6 octahedra share corners to form a three-dimensional framework with the AlO_4^{5-} units filling large voids defined by eight corner-sharing octahedral DBa_6 units. The oxygen tetrahedron surrounding aluminum is nearly regular (Al–O1 = 1.749(2) Å (2×), Al–O2 = 1.773(4) Å, Al–O3 = 1.784(4) Å; angles 107.2(1), 108.1(1), 108.6(2), and 117.5(2)°). The AlO_4^{5-} tetrahedron is surrounded by eleven barium atoms in a peculiar polyhedron (Fig. 5) in which seven barium atoms define a polyhedron that allows the four oxygen vertices of the tetrahedron to lie near the bases of four distorted square pyramids of Ba. This agreement leads to optimized Ba–O and Al–O bond distances and O–Al–O bond angles and reflects the "rigid" or "hard" chemical character of the aluminate anions. On the other hand, the low-field, polarizable deuteride lies in a strongly distorted barium octahedron because it is relatively "anomalous" (21) or "soft" (22). This also explains why the isotropic thermal parameter of the D atom is relatively large compared with those of the other atoms.

In the Ba_3AlO_4D structure, all three cystallographicaly independent oxygen atoms are octahedrally coordinated to one A1 and five Ba atoms. The average Ba–O bond lengths (2.90 (O1), 2.80 (O2), and 2.83 Å (O3)) are significantly longer than either the sum of crystal radii of Ba^{2+} and O^{2-} (2.70 Å, CN 6) (23) or the mean Ba–O distances in $Ba_{21}Ge_2O_5H_{24}$ and Ba_3GeO (2.73 Å for both). However, bond valence calculations performed with bond length parameters derived by Brese and O'Keeffe (24) show bond orders sums of 1.82 for O1, 2.00 for O2, and 1.95 for O3, close to the expected value of 2.0. The increase of Ba–O distances probably correlates with the presence of the sixth

TABLE 2
Powder Neutron Data Collection and Refinement Parameters for Ba_3AlO_4D

Temperature (°C)	23
Lattice constants (Å)[a]	$a = 10.4911(9)$ $b = 8.1518(7)$ $c = 7.2399(6)$
V(Å^3)	619.2(1)
Number of data	5252
Number of reflections	2865
Variables	42
Residuals; R_p, R_{wp}[b] (%)	3.47, 5.22
χ^2	1.748
Scattering lengths (10^{-12} cm)[c]	Ba, 0.507 Al, 0.346 O, 0.580 D, 0.667

[a] Guinier data.

[b] $R_p = (\sum(|I_o - I_c|)/\sum I_o$; $R_{wp} = [\sum(I_o - I_c)^2/\sum wI_o^2]^{1/2}$.

[c] Reference (23).

TABLE 3
Positional Parameters for Ba_3AlO_4D and Ba_3AlO_4H[a]

Atom	x	y	z	$10^2 U_{iso}$(Å^2)
Ba1	0.3346(1)	0.0259(2)	0.1010(2)	0.14(3)
	0.33497(3)	*0.0251(5)*	*0.10172(7)*	*0.62(2)*
Ba2	0.4625(2)	1/4	0.5990(3)	0.07(4)
	0.46330(5)	*1/4*	*0.5988(1)*	*0.48(2)*
Al	0.1029(3)	1/4	0.3110(5)	0.07(6)
	0.1037(3)	*1/4*	*0.3108(4)*	*0.4(1)*
O1	0.0725(1)	0.0665(2)	0.1938(2)	0.53(3)
	0.0719(4)	*0.0657(6)*	*0.1949(7)*	*1.1(1)*
O2	0.0119(2)	1/4	0.5172(3)	0.37(4)
	0.0116(6)	*1/4*	*0.519(1)*	*0.6(1)*
O3	0.2680(2)	1/4	0.3706(3)	0.46(4)
	0.2673(6)	*1/4*	*0.372(1)*	*1.1(1)*
D	0.2310(2)	1/4	0.8393(3)	1.81(5)

[a] Values in the first line are from refinement of neutron powder data from the deuteride, and those on the second line, from X-ray single-crystal data for the hydride.

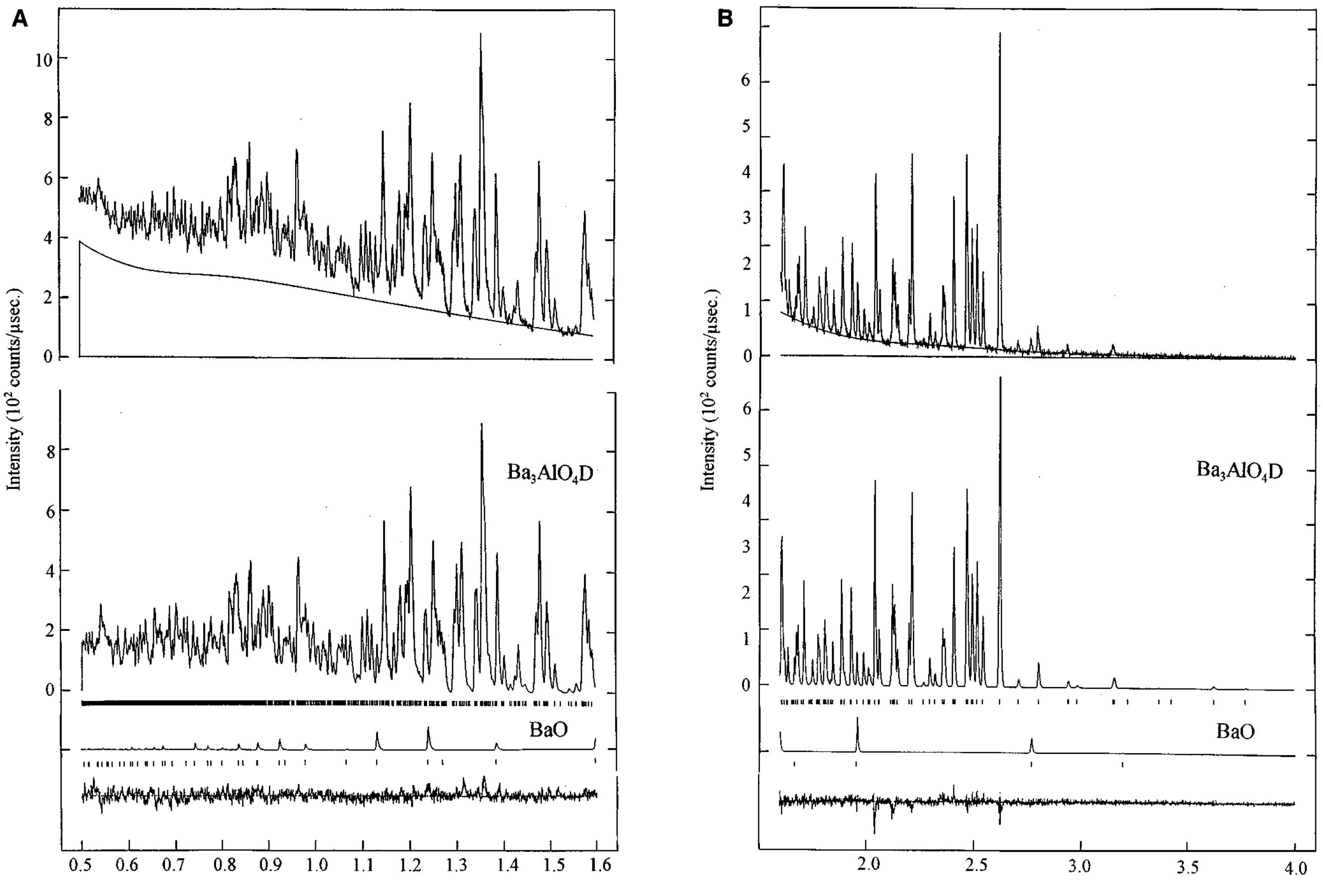

FIG. 1. Neutron powder pattern of Ba_3AlO_4D divided into two regions, $d = 0.5$–1.6 and 1.6–4.0 Å. Shown in each are, from top to bottom, the experimental pattern with fitted background; the calculated patterns for the major and impurity BaO phases and the locations of the reflections used (tick marks); and the difference spectrum on the same scale.

TABLE 4
Important Bond Distances (Å) and angles (Deg) in Ba_3AlO_4D

Ba1–D	2.851(2)	O1–Al	1.749(2)
Ba1–D	2.915(2)	O1–Ba2	2.695(2)
Ba1–O2	2.744(2)	O1–Ba2	2.839(3)
Ba1–O3	2.764(2)	O1–Ba12	2.851(2)
Ba1–O2	2.832(2)	O1–Ba1	2.923(2)
Ba1–O1	2.851(2)	O1–Ba1	3.195(2)
Ba1–O1	2.9223(2)	O2–Al	1.773(4)
Ba1–O3	3.000(2)	O2–Ba1 (2 ×)	2.744(2)
Ba1–O1	3.195(2)	O2–Ba1 (2 ×)	2.832(2)
Ba2–D	2.843(3)	O2–Ba2	2.826(3)
Ba2–D	2.995(5)	O3–Al	1.784(4)
Ba2–O3	2.626(3)	O3–Ba2	2.626(3)
Ba2–O1 (2 ×)	2.695(2)	O3–Ba1 (2 ×)	2.764(2)
Ba2–O2	2.826(3)	O3–Bal (2 ×)	3.000(2)
Ba2–O1 (2 ×)	2.839(3)	D–Ba2	2.843(3)
Al–O1 (2 ×)	1.749(2)	D–Ba1 (2 ×)	2.851(2)
Al–O2	1.773(4)	D–Ba1 (2 ×)	2.915(2)
Al–O3	1.784(4)	D–Ba2	2.995(3)
O1–Al–O1	117.5(2)	Ba1–D–Ba1	79.69(7)
O1–Al–O2	108.1(1)	Ba1–D–Ba2	81.12(6)
O1–Al–O3	107.2(1)	Ba1–D–Ba2	82.13(6)
O2–Al–O3	108.6(2)	Ba1–D–Ba1	89.34(2)
		Ba1–D–Ba2	94.17(7)
		Ba1–D–Ba1	100.99(8)
		Ba1–D–Ba2	106.00(7)

high-field Al^{3+} neighbor. Calculations on the deuterium site gave bond orders of 0.18 (2 ×), 0.15 (2 ×) (Ba1–D), and 0.19 and 0.12 (Ba2–D) and a bond order sum about deuterium of 0.97, close to the ideal value of 1.0. Finally, an oxidation state count indicates Ba_3AlO_4H is a valence compound, as supported by its transparency.

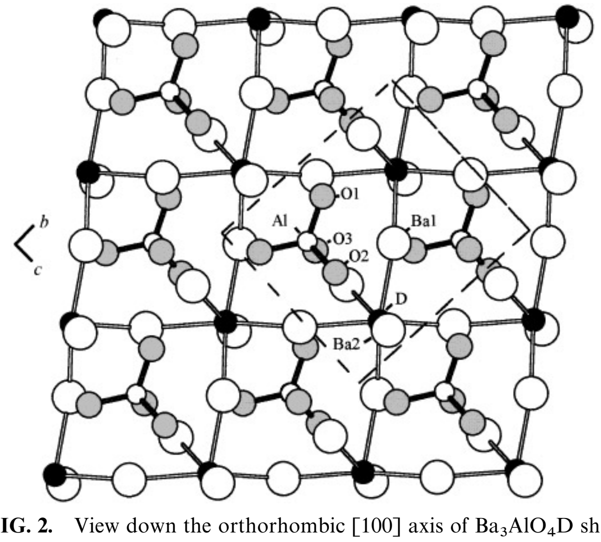

FIG. 2. View down the orthorhombic [100] axis of Ba_3AlO_4D showing the DBa_6 octahedra sharing corners to form a network.

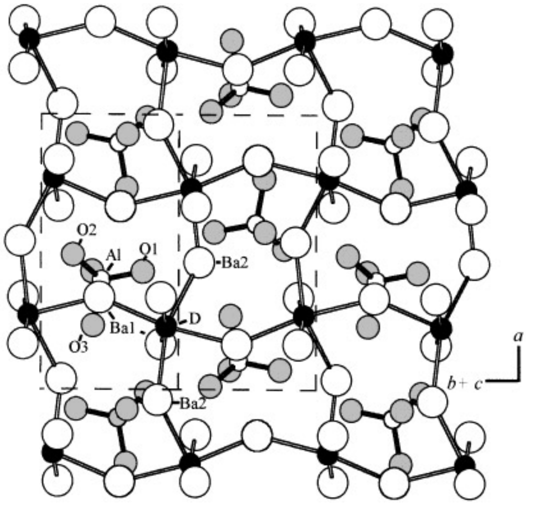

FIG. 3. [01$\bar{1}$] view of Ba_3AlO_4D showing the network of corner-sharing DBa_6 octahedra.

In comparison, Ba_3GeO crystallizes in the orthorhombic inverse perovskite $GdFeO_3$ type (24) with the same space group, *Pnma* (13). The slightly deformed corner-sharing OBa_6 octahedra here make up a three-dimensional framework, and Ge atoms are bound in barium voids that are defined by eight OBa_6 units. This structure is similar to that of Ba_3AlO_4D except for the stacking of X_3A since the difference in formal charge between the Ge^{4-} and AlO_4^{5-} anions is just compensated by the charge difference between divalent oxygen and monovalent deuterium. In the structure of Ba_3AlO_4D, the larger AlO_4^{5-} complex anion with only near-tetrahedral, not spherical, symmetry causes a strong deformation of the cubic-close-packed arrangement. It is interesting that reduced charges on both the cations ($A = \mathrm{K, Rb, Cs}$) and MnX_4^{2-} tetrahedra ($X = \mathrm{Cl, Br, H}$) make the related $A_3(MnX_4)X$ phases tetragonal ($I4/mcm$) with linear chains of elongated A_6H octahedra (26).

There is also as series of basic orthosilicates $(A^{II})_3O(SiO_4)$ for $A = \mathrm{Ca, Sr, Ba, Cd}$, etc. that contain the same type of

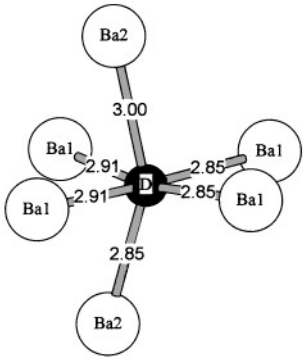

FIG. 4. Environment around the deuterium atom in Ba_3AlO_4D.

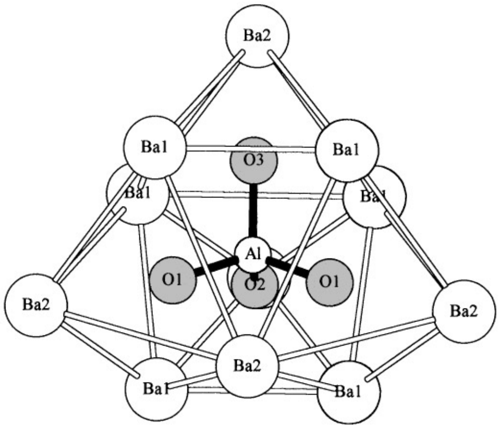

FIG. 5. The tetrahedral AlO_4^{5-} anion and its barium neighbors.

components as does $Ba_3H(AlO_4)$. Several are polymorphic. Those closest in cation size, the strontium (27) and barium (28) salts, have primitive and centered tetragonal structures, respectively, but no orthorhombic examples seem to be known. This general contrast with the structure of Ba_3AlO_4H seems to be a logical consequence of the presence of the hard oxide instead of the lower charged, polarizable hydride. For example, the barium coordination by oxygen changes from 10 and 8 in the oxide, two each involving the lone oxygen atom ($4/m$), to six oxygen (on the AlO_4^{5-}) and two hydrogen in the present case. The lower symmetries about both the lone anion and the MO_4 group are clear (Figs. 4 and 5) and the polyoxoanion is also more distorted.

ACKNOWLEDGMENTS

We are indebted to S. Short and J. Jorgensen for provision of the neutron diffraction data. This research has benefited from the use of the Intense Pulsed Neutron Source at Argonne National Laboratory, which is funded by the U.S. Department of Energy, BES-Materials Sciences, under Contract W-31-109-ENG-38.

REFERENCES

1. E. A. Leon-Escamilla and J. D. Corbett, *J. Alloys Compd.* **206,** L15 (1994).
2. E. A. Leon-Escamilla and J. D. Corbett, *J. Alloys Compd.* **265,** 105 (1998).
3. E. A. Leon-Escamilla, Ph.D. Dissertation, Iowa State University, 1996.
4. R. W. Henning, E. A. Leon-Escamilla, J.-T. Zhao, and J. D. Corbett, *Inorg. Chem.* **36,** 1282 (1997).
5. B. Huang and J. D. Corbett, *Inorg. Chem.* **37,** 1892 (1998).
6. G. D. Brunton and H. Steinfink, *Inorg. Chem.* **10,** 2301 (1971).
7. A. Bruzzone, E. Franceschi, and F. Merlo, *J. Less-Common Met.* **60,** 59 (1978).
8. M. L. Fornasini and M. Pani, *J. Alloys Compd.* **205,** 179 (1994).
9. M. L. Fornasini and F. Merlo, *Rev. Chim. Miner.* **16,** 458 (1979).
10. C. Röhr, *Z. Anorg. Allg. Chem.* **621,** 1496 (1995).
11. C. Röhr, *Z. Kristallogr.*, Suppl. Issue No. 9, 24 (1995).
12. C. Röhr and R. George, *Angew. Chem., Int. Ed. Engl.* **34,** 2115 (1995).
13. B. Huang and J. D. Corbett, *Z. Anorg. Allg. Chem.* **324,** in press (1998).
14. P. Appendino, *Ann. Chim,* (*Rome*) **61,** 822 (1971).
15. G. M. Sheldrick, SHELXS-86, Universtät Göttingen, Göttingen, Germany, 1986.
16. TEXSAN, Version 6.0, Molecular Structure Copr., The Woodlands, TX, 1990.
17. N. Walker and D. Stuart, *Acta Crystallogr., Sect. A* **39,** 158 (1983).
18. H. M. Rietveld, *Acta Crystallogr.* **22,** 151 (1967).
19. A. C. Larson and R. B. Von Dreele, Report LAUR 86-748; Los Almos National Laboratory, Los Almos, NM, 1995.
20. V. F. Sears, *Neutron News* **3,** 26 (1992).
21. W. Bronger, *Angew. Chem., Int. Ed. Engl.* **30,** 759 (1991).
22. K. Yvon, *in* "Encyclopedia of Inorganic Chemistry" (R. B. King, Ed.), Vol. 3, p. 1401. Wiley, New York, 1994.
23. R. D. Shannon, *Acta Crystallogr., Sect. A* **32,** 751 (1976).
24. N. E. Brese and M. O'Keeffe, *Acta Crystallogr., Sect. B* **47,** 192 (1991).
25. S. Geller, *J. Chem. Phys.* **24,** 1236 (1956).
26. W. Bronger, S. Hasenberg, and G. Auffermann, *J. Aloys. Compd.* **257,** 75 (1997).
27. W. Eysel, *Neues Jahrb. Mineral. Monatsh.* 534 (1970).
28. E. Tillmanns and H.-P. Grosse, *Acta Crystallogr., Sect. B* **34,** 649 (1978).